An Efficient Approach for Eikonal-Based Cardiac Activation Site Localization

Ingmar F Lercher[1], Elena Zappon[2], Matthias A F Gsell[2], Thomas Pock[1,2,3], Gernot Plank[2,3]

[1] Graz University of Technology, Graz, Austria
[2] Gottfried Schatz Research Center for Cell Signaling, Metabolism and Aging – Division of Biophysics, Medical University of Graz, Graz, Austria
[3] BioTechMed-Graz, Graz, Austria

Abstract

Cardiac digital twins of human electrophysiology hold significant promise for clinical applications enabling precision therapy. However, calibrating them to patient data at clinical-resolution meshes remains impractically slow, with existing methods requiring hours per calibration. We present an eikonal-based calibration approach that utilizes an exact parameter update, while sharply cutting computation time as well as memory consumption, which enables calibration on consumer-grade GPUs. On a biventricular mesh of $2.1\,M$ *elements with 12-lead ECG recordings the method converged in roughly* $6.7\,\mathrm{min}$ *at a* $2.2\,\mathrm{GB}$ *working memory peak on a Nvidia TITAN RTX.*

1. Introduction

Cardiac digital twins are physics-based virtual representations of an individual patient's heart. By reproducing patient-specific cardiac function, these models could support diagnosis and predict responses to therapeutic interventions and thereby inform treatment planning. Realizing this potential requires calibrating the governing model parameters so that simulated behavior is consistent with the physics of a patient heart. However, calibration is particularly challenging in cardiac electrophysiology. The dynamics of electric sources within the myocardium cannot generally be observed directly; instead, measurements provide only sparse samples of the extracellular potential fields they generate. Constraining a digital twin governed by a large spatially heterogeneous parameter space with sparse indirect observations constitutes a high-dimensional, ill-posed inverse problem.

The ventricular cycle begins with electrical activation: the Purkinje network excites the myocardium at focal *earliest activation sites* (EAS) Θ, initiating wavefront propagation at specific locations and onset time points governed by the spatially varying conduction velocity, $CV(\mathbf{x})$ and anisotropy, α. The resulting arrival times, described by the eikonal model [1], determine the cardiac sources underlying the ECG QRS complex. These sources can be reconstructed from the arrival times and mapped to the ECG through a lead-field formulation [2, 3]. Calibrating ventricular activation therefore amounts to identifying the depolarization parameters $\boldsymbol{\omega}_{\mathrm{D}} = CV(\boldsymbol{x}), \alpha, \Theta$ by minimizing the discrepancy between predicted and observed QRS complexes. In this work we only focus on the earliest activation sites Θ.

Identifying these parameters from observed ECG recordings — calibrating the digital twin — amounts to solving an inverse problem. Existing methods differ in how the parameters Θ are updated to minimize the discrepancy. In GEASI [4] the parameter update involves solving ordinary differential equations (ODEs), which took $18\,\mathrm{h}$ to fit the ECG on a 1.08×10^5-DOF biventricular model using an Nvidia RTX 2080. In the geodesic backpropagation approach [5], fixed-point iteration updates are tracked (loop unrolling) and automatic-differentiation (AD) is used to update the parameters. This approach is faster than GEASI's ODE-based update — 1.8 h on a 2.5 M-element tetrahedral mesh using a 48 GB Nvidia A100 — but requires significantly more GPU memory due to loop unrolling. What remains missing is a formulation for updating Θ that stays low in runtime and memory alike.

Our contribution is a formulation for updating Θ that is memory efficient (no loop unrolling), cheap to compute (no ODEs to solve) and therefore compatible with consumer-grade GPUs and agnostic to the eikonal solver. It requires only the converged eikonal solution and the calculated per-node stencil weight matrix of the mesh.

On a $2.1\,$M-element biventricular mesh (referred to as $\mathcal{M}$ throughout) the closed-form backward pass (parameter update) runs in $37\,\mathrm{ms}$ at $2.2\,\mathrm{GB}$ memory. A full 1000-iteration calibration converged in $\approx 6.7\,\mathrm{min}$ on a 24GB Nvidia TITAN RTX

2. Methods

In this section we introduce the forward model, the inverse problem and describe how we apply the implicit function theorem [6] and the envelope theorem [7] to derive an efficient formulation for the parameter update.

2.1. Forward model

Let $\Omega_h \subset \mathbb{R}^3$ be a tetrahedral heart mesh with N_v vertices $\boldsymbol{v} \in \mathbb{R}^3$ and let $\Theta = \{(\boldsymbol{x}_i, t_i) \in \Omega_h \times \mathbb{R}_+\}_{i=1}^K$ denote the K earliest activation sites. The forward ECG model

$$\hat{u} = (\mathcal{H} \circ \mathcal{E} \circ \mathcal{S})(\Theta), \qquad \Theta \xmapsto{\mathcal{S}} \phi_0 \xmapsto{\mathcal{E}} \phi \xmapsto{\mathcal{H}} \hat{u}$$

maps Θ to an N_l-channel ECG of N_t time-steps, $\hat{u} \in \mathbb{R}^{N_l \times N_t}$, through three operators. The seeding operator $\mathcal{S}$ discretizes $(\boldsymbol{x}_i, t_i)$ by initializing the arrival times at the vertices of the *enclosing* tetrahedron as $(\phi_0)_{\boldsymbol{v}} = t_i + \|\boldsymbol{v} - \boldsymbol{x}_i\|_M$ and $+\infty$ otherwise, with metric $M = D^{-1}$, which stores the conduction velocities and fiber directions, where $D \in \mathbb{R}^{3\times 3}_{\text{sym}}$ is in general a symmetric and positive definite matrix. The eikonal operator maps the initial arrival time field ϕ_0 to the *converged* endstate ϕ by solving $\sqrt{\nabla\phi^\top D\,\nabla\phi} = 1$ in Ω_h where $\phi(\boldsymbol{v}) = (\phi_0)_{\boldsymbol{v}}$. To complete the forward model the operator $\mathcal{H}$ maps ϕ to the ECG by utilizing the lead-field approach [2, 3], $\hat{u}_\ell(t) = \int_{\Omega_h} \langle \sigma_i \nabla V_m, \nabla Z_\ell \rangle \,\mathrm{dx}$ with intracellular conductivity $\sigma_i \in \mathbb{R}^{3\times 3}$, lead-field $Z_\ell \in \mathbb{R}^{N_v}$ and action-potential $V_m(\boldsymbol{x}, t) = U(t - \phi(\boldsymbol{x})) \in \mathbb{R}$, summarized as $\mathcal{H}(\phi) = W_{\text{ECG}}\, V(\phi)^\top$ where $V(\phi) \in \mathbb{R}^{N_t \times N_v}$ is the action-potential over all time-steps of ϕ and $W_{\text{ECG}} \in \mathbb{R}^{N_l \times N_v}$ is the lead-field matrix that is built from the finite-element stiffness matrix and weighted by Z_ℓ and σ_i

2.2. Inverse problem

The objective of the inverse problem is to minimize the misfit between the calculated ECG $\hat{u}$ and the ground truth ECG $u^* \in \mathbb{R}^{N_\ell \times N_t}$, which is achieved by minimizing the nonlinear least-squares problem w.r.t. Θ

$$\min_{\Theta}\; L(\Theta) = \tfrac{1}{2N_\ell}\, \|r(\Theta)\|^2,$$

with the residual $r(\Theta) = \hat{u}(\Theta) - u^*$, where each earliest activation site $(\boldsymbol{x}_i, t_i) \in \Theta$ is restricted to $\Omega_h \times \mathbb{R}_+$. Solving the inverse problem with a gradient-based approach requires the eikonal Jacobian $J_{\mathcal{E}} := \partial\phi/\partial\phi_0$, which is not trivially computable. We derive this Jacobian by applying the envelope theorem to the discrete Hopf-Lax formula [8] for tetrahedral elements in combination with the implicit function theorem. We first state the nodal update and explain the application of the envelope theorem afterwards.

Let $\boldsymbol{v}_k$ be the vertex whose activation time is currently being updated in the eikonal solver and let $\mathcal{N}_k$ be the set of all tetrahedral elements in Ω_h adjacent to the vertex $\boldsymbol{v}_k$. Suppose that, for each tetrahedron $\tau = \operatorname{conv}\{\boldsymbol{v}_{l_0}, \boldsymbol{v}_{l_1}, \boldsymbol{v}_{l_2}, \boldsymbol{v}_{l_3}\} \in \mathcal{N}_k$ the local index l_0 maps to the global index k such that $\boldsymbol{v}_{l_0} = \boldsymbol{v}_k$ and the opposite face is given by $F = \operatorname{conv}\{\boldsymbol{v}_{l_1}, \boldsymbol{v}_{l_2}, \boldsymbol{v}_{l_3}\}$, carrying activation times $\phi|_F$. To find the arrival time for vertex $\boldsymbol{v}_k$, the following minimization problem has to be solved [8]

$$\phi(\boldsymbol{v}_k) = \min_{\tau \in \mathcal{N}_k} \underbrace{\left(\min_{\alpha \in \Delta_F} \underbrace{\Big(\langle \alpha, \phi|_F \rangle + \|A_\tau \alpha\|_2 \Big)}_{G_k^\tau(\alpha, \phi|_\tau)} \right)}_{\Psi_k^\tau(\phi|_\tau)}$$

with $A_\tau = M^{1/2} E_\tau$, edge matrix $E_\tau = (\boldsymbol{v}_{l_1} - \boldsymbol{v}_k, \boldsymbol{v}_{l_2} - \boldsymbol{v}_k, \boldsymbol{v}_{l_3} - \boldsymbol{v}_k) \in \mathbb{R}^{3\times 3}$ and the probability simplex Δ_F for face F. At convergence $\phi_k^* = \phi^*(\boldsymbol{v}_k) = G_k^{\tau^*}(\alpha^*(\phi|_{\tau^*}), \phi|_{\tau^*})$ and differentiating w.r.t. a nodal value $\phi_j = \phi(\boldsymbol{v}_j)$ where $\boldsymbol{v}_j \in F$ the α^*-term vanishes by the envelope theorem [7]

$$\frac{\partial \phi_k^*}{\partial \phi_j} = \underbrace{\frac{\partial G_k^{\tau^*}}{\partial \alpha}\Big|_{\alpha^*} \frac{\partial \alpha^*}{\partial \phi_j}}_{=0} + \frac{\partial G_k^{\tau^*}}{\partial \phi_j} = (\alpha_k^*)_j =: W_{kj}. \quad (1)$$

A vertex k seeded by $(\boldsymbol{x}_i, t_i)$ that keeps its onset time as the earliest arrival time corresponds to a zero row in the *stencil weight matrix* $W \in \mathbb{R}_+^{N_v \times N_v}$, i.e. $W_{kj} = 0$. Once the vertex is overshadowed, i.e. t_i exceeds the arrival time of the eikonal solution, it is treated as a non-seeded vertex and $(\boldsymbol{x}_i, t_i)$ then receive no gradient. We record this split in the diagonal indicator matrix $\mathcal{I} = \operatorname{diag}(\iota) \in \{0,1\}^{\mathrm{N_v} \times \mathrm{N_v}}$, where $\iota_k = 1$ if vertex k remains seeded and $\iota_k = 0$ if it is overshadowed.

2.3. Closed-form gradient derivation

The residual r is backpropagated through the forward model by reverse-mode differentiation. The gradient is the vector–Jacobian product chain $\nabla_\Theta L = J_{\mathcal{S}}^\top J_{\mathcal{E}}^\top J_{\mathcal{H}}^\top r \in \mathbb{R}^P$ evaluated right to left, with $J_{\mathcal{S}} = \partial\phi_0/\partial\Theta$, $J_{\mathcal{E}} = \partial\phi/\partial\phi_0$ and $J_{\mathcal{H}} = \partial\hat{u}/\partial\phi$.

The ECG cotangent is explicit from the compact matrix-matrix formulation, i.e. $g_\phi := \frac{1}{N_\ell} J_{\mathcal{H}}^\top r = -\frac{1}{N_\ell} \sum_{j=1}^{N_t} U'(t_j\, \mathbf{1} - \phi) \odot (W_{\text{ECG}}^\top r_j)$ with r_j the residual at time j and U' the action-potential derivative.

The eikonal cotangent arises from pulling back the ECG cotangent, i.e. $g_{\mathcal{E}} = J_{\mathcal{E}}^\top g_\phi$. This can be done without explicitly forming the eikonal Jacobian by differentiating the implicit function that the arrival-time field fulfills at convergence (no loop unrolling)

$$\hat{\Psi}(\phi, \phi_0) := W\phi + c(W) + \mathcal{I}\phi_0, \quad (2)$$

with $c(W)$ representing the norm term w.r.t ϕ_0 where the eikonal Jacobian follows by (1) as $J_{\mathcal{E}} = (I - W)^{-1}\mathcal{I}$. We

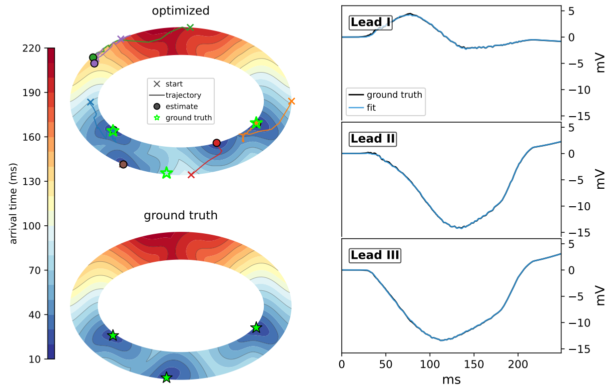

Figure 1. Synthetic 2D experiment. Top: the optimized EAS closely matches the ground truth arrival-time field. Bottom: the recovered ECG (only I - III are shown) in blue matches the synthetic target in black.

avoid the matrix inversion by solving an adjoint system $(I - W^\top)\lambda = g_\phi$ for λ first and construct the cotangent as $g_\mathcal{E} = \mathcal{I}\lambda$

The trivial seeding Jacobian $J_\mathcal{S}$ is nonzero only on the vertices $\boldsymbol{v}$ of the tetrahedron τ that contains $\boldsymbol{x}_i$ with the gradients for t_i and $\boldsymbol{x}_i$ as $\frac{\partial L}{\partial t_i} = \sum_{\boldsymbol{v}\in\tau}(g_\mathcal{E})_{\boldsymbol{v}}$ and $\frac{\partial L}{\partial \boldsymbol{x}_i} = -\sum_{\boldsymbol{v}\in\tau}(g_\mathcal{E})_{\boldsymbol{v}} \frac{M_\tau(\boldsymbol{x}_{\boldsymbol{v}}-\boldsymbol{x}_i)}{\|\boldsymbol{x}_{\boldsymbol{v}}-\boldsymbol{x}_i\|_{M_\tau}}$ respectively.

2.4. Benchmark & Experiments

We evaluate i) the ability of our inverse model to optimize location and timing of earliest activation sites Θ to minimize the mismatch to a target ECG and ii) measure the iteration time (forward + backward pass), the backward pass time separately as well as the memory allocation. Two experimental setups of increasing complexity have been considered. The *first experiment* demonstrates the correctness our approach by fitting an ECG of a heart slice (12 cm $\times$ 8 cm) embedded in a 2D heart-torso model (30 cm $\times$ 20 cm). We set 3 ground truth source points, $K = 6$ evenly placed initial EAS and calculated 6 lead-fields from the synthetic model. (Fig. 1). In a *second experiment* we used a previously generated anatomical heart and torso model of a healthy adult male [9], comprising a biventricular mesh $\mathcal{M}$ of 2.1 M elements conformally embedded in a torso mesh elements over which all lead-fields of a Mason-Likar electrode placement were precomputed to recover a clinical 12-lead ECG. The number of EAS $|\Theta|$ was set to an arbitrary number of $K = 100$, which were evenly distributed over the mesh with random onset times in a 200 ms to 350 ms range and focused on the QRS complex over a 200 ms window at a 1.0 ms resolution. The ECG was computed with a chunk size of 32 over the time dimension and we compared the iteration time, the backward pass time and the GPU memory allocation of

Table 1. Computational costs averaged over 10 iterations for $\mathcal{M}$ with 100 EAS. Numbers are reported at an ECG time-chunk of 32. The memory allocation is measured with the torch `max_allocated` function; the total process footprint is larger and depends on the CUDA caching-allocator configuration and the eikonal solver iself.

	AD (naive)	AD (opt.)	Ours
Backward pass	382 ms	97 ms	37 ms
Iteration time	1.05 s	0.48 s	0.40 s
Alloc. GPU memory	15.3 GB	2.3 GB	2.2 GB

our method against two automatic-differentiation baselines an optimized one using PyTorch's just-in-time compilation and a non-optimized naive one – both variants only back-propagate $r(\Theta)$ through $\mathcal{H}$ via AD. In an *isolated benchmark* test the scalability of the backward pass time of the closed-form and the optimized AD variant with $|\Theta| = 100$ at different chunk sizes was investigated on $\mathcal{M}$.

All experiments were conducted on a 24 GB Nvidia TITAN RTX GPU and used the L-BFGS method to update Θ and solved the eikonal equation with a GPU-accelerated Fast Iterative Method [10] tailored to the inverse problem.

3. Results

In the first experiment a near-perfect match of the entire QRS complex of the ECG was achieved (see Fig. 1). The left and right ground truth EASs were exactly recovered (blue and orange EAS), whereas the EASs in the middle was not recovered. The green and purple EASs were overshadowed.

Evaluation of computational costs in experiment 2 using $\mathcal{M}$ showed that our closed-form backward pass took 37 ms, the optimized AD and the naive AD variants took 97 ms and 382 ms respectively. The peak GPU memory consumption of our closed-form and the optimized AD variants were comparable at $\approx$2.2 GB whereas the naive variant required 15.3 GB. Furthermore, using our approach, 1000 L-BFGS iterations took $\approx$6.7 min and converged to a loss of $\approx$0.4 resulting in an recovered ECG that closely matches the target over the QRS window (Fig. 2). From the original 100 EAS only two were overshadowed.

An isolated benchmark showed that the closed-form gradient scales well with the number of ECG time-steps, outperforming the opt. AD variant by up to 5$\times$ (Tab. 2).

4. Discussion

Our optimization method successfully identified EASs that produced activation sequences yielding near-perfect agreement with the target ECG in both benchmarks. In the simple benchmark, the ground-truth activation pattern was also recovered with high accuracy; this was not assessed

Table 2. Backward pass time (ms) on $\mathcal{M}$ as the ECG horizon N_t grows.

N_t	chunk	Ours	AD (opt.)	speedup
256	32	36	113	3.1×
	64	36	106	2.9×
	N_t	36	106	3.0×
512	32	40	199	5.0×
	64	40	188	4.7×
	N_t	39	186	4.7×

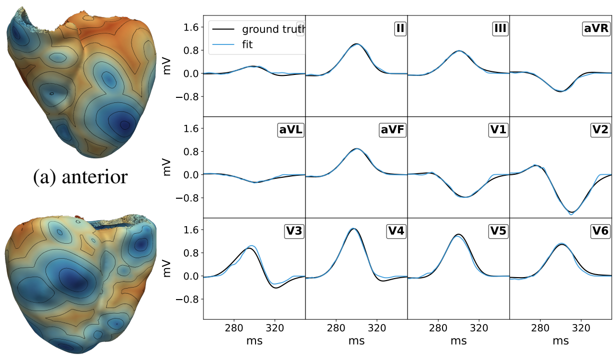

(a) anterior

(b) posterior

(c) recovered vs. target ECG

Figure 2. Result of experiment 2 with $|\Theta| = 100$. (a,b) anterior and posterior views of the reconstructed arrival-time field; (c) the recovered (blue) and the ground truth (black) 12-lead ECG over the $250\,\mathrm{ms}$ to $350\,\mathrm{ms}$ QRS window.

in the biventricular benchmark as the activation sequence is not known. Previous studies have shown that this inverse problem is non-unique, as multiple – and potentially many – distinct sets of EASs may produce indistinguishable ECGs [5]. Consequently, agreement with the target ECG does not necessarily imply recovery of the underlying activation pattern. A systematic analysis of identifiability, however, was beyond the scope of this study.

In our approach we combined implicit differentiation with the envelope theorem to derive an efficient formulation that yields low iteration times at low memory consumption on a consumer-grade GPU, enabling the optimization a set of EAS that reproduce a given ECG within minutes.

The closed-form gradient extends to optimizing conduction velocities and we expect it to further outperform the AD variant in that setting.

5. Conclusion

In this work we derived an efficient method for eikonal-based calibration of cardiac digital twins in less than $10\,\mathrm{min}$. Future studies should address optimizing conduction velocities as well as the non-uniqueness of the inverse problem.

Acknowledgments

This work was funded by the Austrian Science Fund (FWF). Grant DOI 10.55776/I6540 awarded to Dr. Gernot Plank.

References

[1] Colli Franzone P, Guerri L, Rovida S. Wavefront propagation in an activation model of the anisotropic cardiac tissue: asymptotic analysis and numerical simulations. Journal of Mathematical Biology 1990;28(2):121–176.

[2] Geselowitz DB. On the theory of the electrocardiogram. Proceedings of the IEEE 1989;77(6):857–876.

[3] Pezzuto S, Kal'avský P, Potse M, Prinzen FW, Auricchio A, Krause R. Evaluation of a rapid anisotropic model for ECG simulation. Frontiers in Physiology 2017;8:265.

[4] Grandits T, Effland A, Pock T, Krause R, Plank G, Pezzuto S. GEASI: Geodesic-based earliest activation sites identification in cardiac models. International Journal for Numerical Methods in Biomedical Engineering 2021;37(8):e3505.

[5] Grandits T, Verhülsdonk J, Haase G, Effland A, Pezzuto S. Digital twinning of cardiac electrophysiology models from the surface ECG: A geodesic backpropagation approach. IEEE Transactions on Biomedical Engineering 2024;71(4):1281–1292.

[6] Blondel M, Berthet Q, Cuturi M, Frostig R, Hoyer S, Llinares-Lopez F, Pedregosa F, Vert JP. Efficient and modular implicit differentiation. In Advances in Neural Information Processing Systems (NeurIPS), volume 35. 2022; .

[7] Danskin JM. The theory of max-min, with applications. SIAM Journal on Applied Mathematics 1966;14(4):641–664.

[8] Bornemann F, Rasch C. Finite-element discretization of static Hamilton–Jacobi equations based on a local variational principle. Computing and Visualization in Science 2006;9(2):57–69.

[9] Gillette K, Gsell MAF, Prassl AJ, Karabelas E, Reiter U, Reiter G, Grandits T, Payer C, Štern D, Urschler M, Bayer JD, Augustin CM, Neic A, Pock T, Vigmond EJ, Plank G. A Framework for the generation of digital twins of cardiac electrophysiology from clinical 12-leads ECGs. Medical image analysis July 2021;71:102080. ISSN 1361-8423.

[10] Fu Z, Kirby RM, Whitaker RT. A fast iterative method for solving the eikonal equation on tetrahedral domains. SIAM Journal on Scientific Computing 2013;35(5):C473–C494.

Address for correspondence:

Ingmar F. Lercher
Graz University of Technology, Graz, Austria
E-mail: ingmar.lercher@tugraz.at